X-ray absorption *K* edge as a diagnostic of the electronic temperature in warm dense aluminum

F. Dorchies,[1,*] F. Festa,[2,3] V. Recoules,[3] O. Peyrusse,[1] A. Benuzzi-Mounaix,[2] E. Brambrink,[2] A. Levy,[2,†] A. Ravasio,[2]
M. Koenig,[2] T. Hall,[4] and S. Mazevet[5]

[1]*Université de Bordeaux, CNRS, CEA, Centre Lasers Intenses et Applications, UMR 5107, F-33400 Talence, France*
[2]*Ecole Polytechnique, Laboratoire d'Utilisation des Lasers Intenses, UMR 7605, F-91128 Palaiseau, France*
[3]*CEA-DAM-DIF, F-91297 Arpajon, France*
[4]*Department of Physics, University of Essex-Colchester, United Kingdom*
[5]*LUTH, Observatoire de Paris, CNRS, Université Paris Diderot, 92195 Meudon Cedex, France*

The use of the x-ray absorption *K*-edge slope is investigated as a model-free diagnostic of the electronic temperature in warm dense matter. Data are reported for aluminum in a wide domain of densities (approximately one to three times the solid density) and temperatures ($\sim$0.1–10 eV). Measurements are obtained from laser-shock compression where both temperature and density are independently determined from optical diagnostics. They are compared with two different theoretical approaches, respectively, based on quantum molecular dynamics and multiple scattering. Extrapolation for other absorption edges and materials is discussed.

PACS number(s): 52.50.Lp, 32.30.Rj, 52.25.Os, 52.27.Gr

The study of warm dense matter (WDM) is one of the great identified challenges of contemporary physics, noticeably driven by its implication to inertial confinement fusion and planetary interiors [1–3].

Past decades have seen important advances both on the experimental and on the theoretical sides. Today laser-shock techniques and associated diagnostics to reach and study the equation of state (EOS) at pressures exceeding the Mbar level are a well-established tool for WDM characterization. On the theoretical side, *ab initio* simulations [4] have given a sophisticated input for available EOS models. Despite this, one crucial point concerns a precise determination of the temperature. This last one is particularly crucial in the sense that it is the parameter on which the discrepancy between currently available EOS models [5,6] is the most important. Usually, in many experiments, shock velocities in two materials (one of reference) can be measured with good precision using viable diagnostics. Then pressure, density, and energy are obtained via the Hugoniot relations [7]. Temperature does not play any role in these equations and must be determined independently. This measurement based on self-emission and reflectivity data is particularly difficult for shocked opaque materials [8]. In nonequilibrium situations, the problem is even more complex since it is essential to specifically determine the electron and/or the ion temperatures that differ [9–11].

X-ray diagnostics have been recently implemented to go beyond the optical measurements. In principle, the temperature can be deduced from the analysis of extended x-ray absorption fine-structure (EXAFS) spectra, but this is limited to quasisolid structures [12]. X-ray scattering has demonstrated the ability to provide density, temperature, ionization state. and ion coupling [13,14]. But the temperature determination is strongly model dependent [15]. Besides this, x-ray absorption near-edge spectroscopy (XANES) gives rich information on

both the local atomic order [16] and the electronic structure that can be strongly changed from solid to WDM [17,18]. This technique probes the electron population close to the Fermi surface, that is directly sculpted by the electron temperature. Considering this, a recent paper limited to the aluminum solid-liquid transition (a fraction of eV) suggested that x-ray absorption edges could be used as a diagnostic of the electronic temperature [19]. In another study [10], higher electron temperatures have been extracted (up to $\sim$1 eV) from Cu L_3-edge XANES spectra, relying on the modeling of the electron density of state.

In this paper, we investigate the possible use of the edge slope of x-ray absorption spectra to get a direct measurement of the electronic temperature. The major interest of such a diagnostic is that it potentially does not depend on any sophisticated model but just on the universal Fermi-Dirac distribution function. *K*-edge spectra of warm dense aluminum are studied in a wide thermodynamical domain ranging from one to three times the solid density and from $\sim$0.1 to 10 eV. Measurements are registered in laser-shock compression experiments with careful optical control of both density and temperature. They are compared with two independent theoretical approaches based on quantum molecular dynamics (QMD) *ab initio* calculations and on finite difference (FD) XANES calculations coupled with a dense plasma model, respectively. We demonstrate that the electronic temperature can be fairly and directly read from the *K*-edge slope from a fraction of eV to $\sim$5 eV, essentially limited by the Fermi energy value. This benefits from the slow varying energy profile of the probed density of state, which is particularly true in simple metals, such as aluminum. The validity of the concept is discussed for other absorption edges and materials.

The x-ray absorption spectrum features near a given edge are dominated by the photoelectric effect coupling a core level with a vacant free-electron state near the continuum. In the case of an absorption *K* edge, the corresponding cross section is given by the following expression:

$$\sigma(h\nu) = ah\nu|\langle\psi_{1s}|R|\psi_f\rangle|^2[1 - f(E)]. \qquad (1)$$

---

*dorchies@celia.u-bordeaux1.fr

†Present address: Sorbonne Universités, UPMC Université Paris 06, UMR 7588, CNRS, INSP, F-75005 Paris, France.
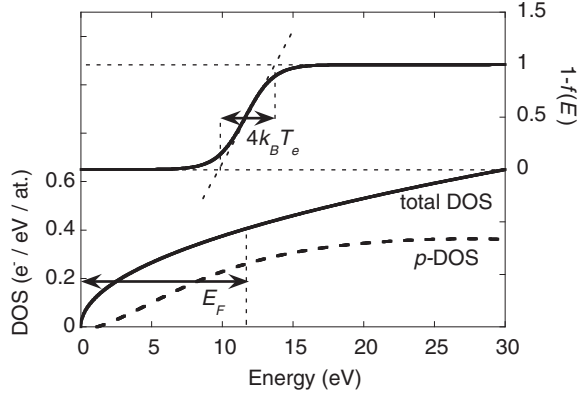
FIG. 1. Compared energy profiles of electronic DOS and the Fermi-Dirac vacancy factor $1 - f(E)$.
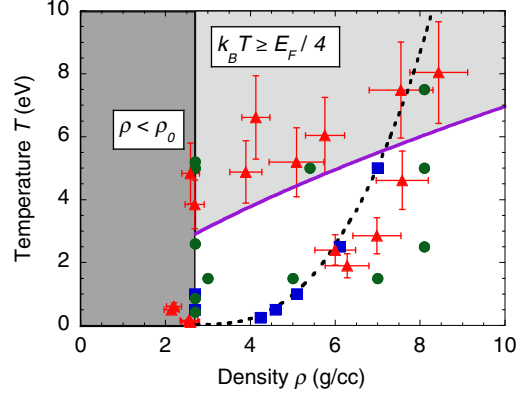

FIG. 2. (Color online) Thermodynamical conditions explored. (*Triangles*) Laser-shock compression measurements. (*Circles*) QMD calculations. (*Squares*) FD calculations. The full line is set to $T = E_F/4$ when the E_F density variation is deduced from the FEG model. (*Dotted line*) Principal Hugoniot.

The $1s$ core level is not significantly affected by the environment, except through screening effects that induce a possible level energy shift [17]. R is the electric dipole moment operator that selects the p states among the final states $|\psi_f\rangle$, and a is a numerical constant. The electronic density of states (DOS) is contained implicitly in the final wave function in the sense that the integration of the square modulus of $|\psi_f\rangle$ over space gives the DOS. Additional effects coming from the local atomic order appear in the form of multiple scattering of $|\psi_f\rangle$ on the nearest-neighboring atoms [20]. The last term $[1 - f(E)]$ is the vacancy factor obtained from Fermi-Dirac statistics. It describes the availability of the final state for the transition. If we can neglect effects from the $|\psi_f\rangle$ phase, then the K-edge absorption spectrum can be estimated from the product of the p-DOS amplitude by the vacancy factor.

The occupation factor $f(E)$ is an intrinsic function of the electronic temperature T_e. As long as $k_B T_e$ is lower than the Fermi energy E_F, electrons are governed by Fermi-Dirac statistics, and $f(E)$ is given by Eq. (2),

$$f(E) = \left[1 + \exp\left(\frac{[E - \mu(T_e)]}{k_B T_e} \right) \right]^{-1}. \quad (2)$$

E is the electron energy. $\mu(T_e)$ is the chemical potential depending also on the electronic temperature and equal to E_F when $T_e = 0$. The vacancy factor $[1 - f(E)]$ is plotted in Fig. 1 for $T_e = 1$ eV at solid density. The slope reaches its maximal value of $(4k_B T_e)^{-1}$ at the inflection point when $E = \mu$. The total DOS is plotted on the same figure when estimated from the free-electron gas (FEG) model that fairly describes the solid aluminum filled up to the Fermi energy $E_F = 11.63$ eV. The p DOS reported in Fig. 1 is set to a function reproducing the general shape of the aluminum DOS projected on p states (see Fig. 5 for calculated p DOS in various conditions). As long as the p DOS can be considered as a slow varying energy profile, the K-edge absorption shape fits with the energy profile of the vacancy factor. Then, the electronic temperature (in fact $4k_B T_e$) can directly be read from the K-edge slope at the inflection point. Note that this determination does not depend on any sophisticated model. Considering Fig. 1, the slow varying p-DOS energy profile assumption can be written as $4k_B T_e \leqslant E_F$. As a consequence,

the direct electronic temperature reading from the K-edge slope should work up to $\sim E_F/4$.

In order to test the validity of such an electronic temperature diagnostic in a wide domain of the WDM phase diagram, we performed measurements and calculations on warm dense aluminum in situations where the temperature was independently determined. Corresponding densities ρ and temperatures T are reported in Fig. 2, typically ranging from solid density ρ_0 (2.7 g/cm^3) up to $3\rho_0$ and from ~ 0 to 10 eV.

Experimental data were obtained using laser-shock compression. The description of the experimental setup, including the compression control and the x-ray absorption spectra recording is detailed in Ref. [17]. To summarize, a high-energy laser pulse (up to 150 J at 532 nm in 500 ps) generates a shock in a multilayer target that compresses the aluminum sample layer. A second laser pulse (20 J at 532 nm in 3.5 ps) is used to produce a synchronized x-ray backlight ($\sim$10-ps duration) that probes the sample with an adjustable delay. Rear-side time-resolved optical diagnostics are used to determine values of density ρ and temperature T when the sample is probed. The (ρ, T) values achieved are plotted in Fig. 2 when the sample is composed of 15-μm plastic (ablator at the laser side), 1-μm aluminum, and 15-μm plastic (rear side). The highest densities are achieved when the sample is probed during its shock compression. When probing after the shock propagation, the temperature remains relatively high ($\sim$5 eV), but the density progressively decreases down to ρ_0. Values higher than the principal Hugoniot have been previously obtained when using a target with a rear-side diamond layer that partially reflects the shock wave [17]. In order to compile data as much as possible, these last measurements are also added in Fig. 2 and considered by the following analysis. In any case, as the shock compression time scale ($\sim$200 ps) is significantly larger than the expected thermal equilibration time (a few picoseconds as can be deduced from Ref. [21]), both electronic and ionic temperatures are supposed to have the same value T.

Two independent theoretical approaches have been considered in order to calculate x-ray absorption spectra. The first is based on QMD *ab initio* calculations, described in detail in Refs. [22,23]. The second is based on real-space FD XANES
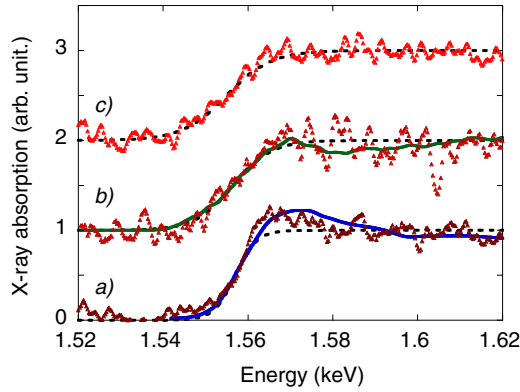
FIG. 3. (Color online) Some x-ray absorption spectra. Measurements are plotted with small triangles. Calculations are indicated with full lines. (a) Measurements at 6.0 ± 0.5 g/cm^3 and 2.4 ± 0.5 eV and FD calculations at 6.1 g/cm^3 and 2.5 eV. (b) Measurements at 7.6 ± 0.6 g/cm^3 and 4.6 ± 0.9 eV and QMD calculations at 8.1 g/cm^3 and 5.0 eV. (c) Measurements at 7.6 ± 0.8 g/cm^3 and 7.5 ± 1.5 eV. The respective Fermi-Dirac fits used to extract the electronic temperature from the measurements are indicated by dashed lines.

calculations coupled with a dense plasma model, described in Ref. [24].

Some measured Al K-edge x-ray absorption spectra are presented in Fig. 3 for three increasing density and temperature conditions near the principal Hugoniot. Two calculated spectra are indicated. They have been performed with thermodynamical conditions comparable with measurements. A fair agreement is observed between measured and calculated spectra. Increasing the temperature from 2.5 to 5 eV reduces the K-edge slope by a factor of 2 as expected from the vacancy factor temperature dependence. Nevertheless, when the temperature reaches 7.5 eV, the slope is not modified so much demonstrating a saturation of the K-edge slope with the temperature.

A simple fitting procedure is used to extract the K-edge maximal slope at the inflection point and the resulting electronic temperature T_e, both on experimental and on calculated spectra. Values obtained are reported in Fig. 4 as a function of the temperature T, which is set to the value deduced from optical diagnostics (experiment) and to the calculations input value, respectively. Vertical error bars come from the fitting procedure. In the case of experimental data, errors in (ρ, T) determination are reported on the horizontal error bars. One can observe a very good determination of the temperature from the K-edge slope for the lowest values of temperature (the full line indicates $T_e = T$). A disagreement progressively appears up to the highest temperature for which T_e is systematically underestimated. The upper limit that guarantees a fair electronic temperature extraction is close to $E_F/4$ as expected from the simple description illustrated in Fig. 1. The corresponding line in the phase diagram is reported in Fig. 2. The validity domain is below this line and covers a wide range of WDM conditions.

In order to assess the pictures sketched in Fig. 1, some DOS calculated from QMD simulations are reported in Fig. 5 for different densities and temperatures representative of the
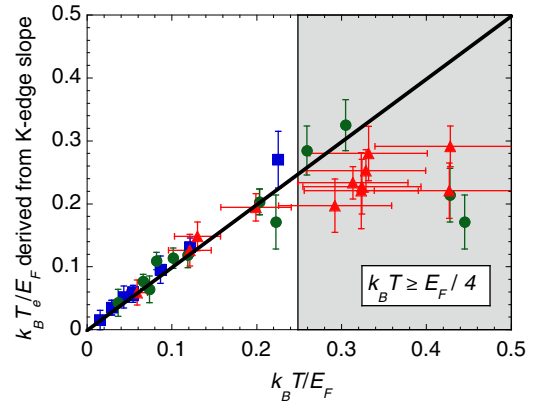

FIG. 4. (Color online) Electronic temperature T_e extracted from the K-edge slope as a function of the temperature T. Symbols are similar to Fig. 2: (*triangles*) measurements, (*circles*) QMD calculations, and (*squares*) FD calculations. T is set to the value deduced from optical diagnostics (experiment) and to the calculation input values, respectively. T_e and T are normalized to the Fermi energy E_F estimated from the FEG model.

phase diagram explored. The total DOS remains very close to the FEG one, and the general shape of the p DOS is essentially unchanged. At the solid density ρ_0 and near the Fermi level, the energy range over which the p DOS varies is close to E_F. At $3\rho_0$, the Fermi level is located further in an energy range where the p DOS is essentially flat. The K-edge slope at the inflection point (corresponding to the Fermi level) should then coincide with the energy slope of the vacancy factor, i.e., $(4k_B T_e)^{-1}$. Nevertheless, at too high temperatures, the low-energy part of the p DOS envelope (first 10 eV in Fig. 5) will necessarily affect the K-edge shape. In both situations, a reasonable limit to read the electronic temperature from the edge is given by $k_B T_e \leqslant E_F/4$. Above, one has to consider the p-DOS energy profile to estimate properly the electronic temperature from the x-ray absorption spectra.

The lower limit of the electron temperature diagnostic is given by the slope of the cold aluminum K-edge spectrum. In
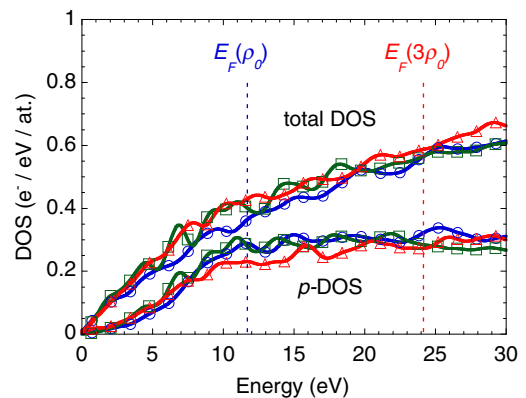

FIG. 5. (Color online) DOS and p DOS calculated by QMD simulations for several values of density and temperature. (*Blue and circles*) 2.7 g/cm^3 and 2.5 eV. (*Green and squares*) 8.1 g/cm^3 and 2.5 eV. (*Red and triangles*) 8.1 g/cm^3 and 7.5 eV. All other density and temperature conditions considered for QMD calculations (circles in Fig. 2) have DOS profiles that overlap well with those shown in this figure.

our experiment, the main contribution comes from the spectral resolution, giving a lower limit of about ~ 0.5 eV for T_e. This could be lowered by improving the x-ray spectrometer setup. Nevertheless, the intrinsic physical limit is given by the core-hole lifetime. It implies a spectral convolution of the Al K edge by a Lorentzian function with $\Gamma = 0.6$-eV full width at half maximum [25], leading to a K-edge slope of $\Gamma \pi / 2 = 0.94$ eV, then a minimal value for $T_e = 0.236$ eV. This lower limit depends on both the edge and the element under consideration [26].

The ability to directly read the electron temperature from the slope of the x-ray absorption edge relies on two general assumptions. The first is to neglect the energy envelope variations in the probed density of states, over an energy range of $4 k_B T_e$. As for aluminum, the DOS of simple metals presents a slow varying energy profile over E_F, that leads to the upper limit $k_B T_e \leqslant E_F / 4$ that we have discussed. The same value is expected when considering other edges than the K edge. The L edge has been already successfully exploited in a low-temperature range ($\leqslant 0.5$ eV) and near solid density [19]. The method can fail when the density goes down the solid one. Indeed, electrons can gradually relocate from the conduction band down to atomic orbitals, severely affecting the DOS profile [18,27]. Other materials, such as transition and noble metals can also be difficult. Their properties are intimately associated with their d bands whose DOS presents a lot of structures. As illustrated in Ref. [10] where the copper d band is especially probed via L_3-edge absorption spectroscopy, the electron temperature extraction from x-ray spectra is still possible but requires precise modeling of the electronic structure. As the p DOS is expected to be less structured than the d one, K-edge spectroscopy could be more suitable to directly extract T_e in a model-free way. The method that we have studied to retrieve T_e is also *a priori* poorly adapted to insulators since the x-ray absorption edge no longer corresponds to the Fermi energy, usually situated in the gap between valence and conduction bands. Nevertheless, in the WDM domain, we could expect that some insulators turn metallic when the temperature increases, possibly extending the use of x-ray absorption edges as T_e diagnostics [28].

The last important assumption consists of neglecting the local order influence. This results in structures in the x-ray absorption spectrum. Among these, EXAFS oscillations should not affect the T_e determination from the edge slope as their typical spectral period is larger than E_F (~ 30 eV for solid aluminum [11]). Nevertheless, some materials can present very sharp spectral structures located near the edge, such as preedge structures or shape resonances (e.g., in tetrahedral systems) [20] that severely constrains the simple use of the edge slope as a direct electron temperature diagnostic.

To summarize, we present a study about the use of x-ray absorption edge spectroscopy to determine the electron temperature T_e in warm dense matter. Experimental and theoretical results are reported for aluminum K-edge spectra in a wide range of densities (from solid ρ_0 to $3\rho_0$) and temperatures (from ~ 0.1 to 10 eV). As a main conclusion, T_e can be directly read from the edge slope in a model-free way as long as $4 k_B T_e$ is lower than the Fermi energy E_F. This limit is understood with a simple picture considering the electron Fermi-Dirac energy distribution near the Fermi surface. The extension of this method is discussed for other edges and materials. Such an electron temperature diagnostic has great potential for the study of WDM, including situations far from the thermal equilibrium where it is of primary importance to have a specific diagnostic of the electron temperature when it differs from the ion temperature.

[1] National Research Council, *Frontiers in High Energy Density Physics: The X-Games of Contemporary Science* (National Academic Press, Washington, D.C., 2003).

[2] G. W. Collins, L. B. Da Silva, P. Celliers, D. M. Gold, M. E. Foord, R. J. Wallace, A. Ng, S. V. Weber, K. S. Budil, and R. Cauble, Science **281**, 1178 (1998).

[3] M. D. Knudson, D. L. Hanson, J. E. Bailey, C. A. Hall, J. R. Asay, and W. W. Anderson, Phys. Rev. Lett. **87**, 225501 (2001).

[4] L. A. Collins, S. R. Bickham, J. D. Kress, S. Mazevet, T. J. Lenosky, N. J. Troullier, and W. Windl, Phys. Rev. B **63**, 184110 (2001).

[5] Los Alamos National Laboratory Report No. LA-UR-92-3407, 1992.

[6] R. M. More, K. H. Warren, D. A. Young, and G. B. Zimmerman, Phys. Fluids **31**, 3059 (1988).

[7] Y. B. Zeldovich and Y. P. Raizer, *Physics of Shock Waves and High Temperature Hydrodynamic Phenomena* (Academic, New York, 1967).

[8] P. Celliers and A. Ng, Phys. Rev. E **47**, 3547 (1993).

[9] R. R. Faüstlin, T. Bornath, T. Döppner, S. Düsterer, E. Förster, C. Fortmann, S. H. Glenzer, S. Göde, G. Gregori, R. Irsig *et al.*, Phys. Rev. Lett. **104**, 125002 (2010).

[10] B. I. Cho, K. Engelhorn, A. A. Correa, T. Ogitsu, C. P. Weber, H. J. Lee, J. Feng, P. A. Ni, Y. Ping, A. J. Nelson, D. Prendergast, R. W. Lee, R. W. Falcone, and P. A. Heimann, Phys. Rev. Lett. **106**, 167601 (2011).

[11] P. M. Leguay, A. Lévy, B. Chimier, F. Deneuville, D. Descamps, C. Fourment, C. Goyon, S. Hulin, S. Petit, O. Peyrusse, J. J. Santos, P. Combis, B. Holst, V. Recoules, P. Renaudin, L. Videau, and F. Dorchies, Phys. Rev. Lett. **111**, 245004 (2013).

[12] Y. Ping, F. Coppari, D. G. Hicks, B. Yaakobi, D. E. Fratanduono, S. Hamel, J. H. Eggert, J. R. Rygg, R. F. Smith, D. C. Swift, D. G. Braun, T. R. Boehly, and G. W. Collins, Phys. Rev. Lett. **111**, 065501 (2013).

[13] A. Ravasio, G. Gregori, A. Benuzzi-Mounaix, J. Daligault, A. Delserieys, A. Y. Faenov, B. Loupias, N. Ozaki, M. Rabec le Gloahec, T. A. Pikuz, D. Riley, and M. Koenig, Phys. Rev. Lett. **99**, 135006 (2007).

[14] S. H. Glenzer, O. L. Landen, P. Neumayer, R. W. Lee, K. Widmann, S. W. Pollaine, R. J. Wallace, G. Gregori, A. Höll, T. Bornath, R. Thiele, V. Schwarz, W.-D. Kraeft, and R. Redmer, Phys. Rev. Lett. **98**, 065002 (2007).

[15] S. H. Glenzer and R. Redmer, Rev. Mod. Phys. **81**, 1625 (2009).

[16] A. Mancic, A. Lévy, M. Harmand, M. Nakatsutsumi, P. Antici, P. Audebert, P. Combis, S. Fourmaux, S. Mazevet, O. Peyrusse, V. Recoules, P. Renaudin, J. Robiche, F. Dorchies, and J. Fuchs, Phys. Rev. Lett. **104**, 035002 (2010).

[17] A. Benuzzi-Mounaix, F. Dorchies, V. Recoules, F. Festa, O. Peyrusse, A. Lévy, A. Ravasio, T. Hall, M. Koenig, N. Amadou, E. Brambrink, and S. Mazevet, Phys. Rev. Lett. **107**, 165006 (2011).

[18] A. Lévy, F. Dorchies, A. Benuzzi-Mounaix, A. Ravasio, F. Festa, V. Recoules, O. Peyrusse, N. Amadou, E. Brambrink, T. Hall, M. Koenig, and S. Mazevet, Phys. Rev. Lett. **108**, 055002 (2012).

[19] K. Oguri, Y. Okano, T. Nishikawa, and H. Nakano, Phys. Rev. Lett. **99**, 165003 (2007).

[20] *X-ray Absorption: Principles, Applications, Techniques of EXAFS, SEXAFS and XANES*, edited by D. C. Koningsberger and R. Prins (Wiley, New York, 1988).

[21] Z. Lin, L. V. Zhigilei, and V. Celli, Phys. Rev. B **77**, 075133 (2008).

[22] S. Mazevet and G. Zerah, Phys. Rev. Lett. **101**, 155001 (2008).

[23] V. Recoules and S. Mazevet, Phys. Rev. B **80**, 064110 (2009).

[24] O. Peyrusse, High Energy Density Phys. **6**, 357 (2010).

[25] O. Peyrusse, J. Phys.: Condens. Matter **20**, 195211 (2008).

[26] P. H. Citrin, G. K. Wertheim, and M. Schlüter, Phys. Rev. B **20**, 3067 (1979).

[27] F. Dorchies, A. Lévy, C. Goyon, P. Combis, D. Descamps, C. Fourment, M. Harmand, S. Hulin, P. M. Leguay, S. Petit, O. Peyrusse, and J. J. Santos, Phys. Rev. Lett. **107**, 245006 (2011).

[28] A. Denoeud, A. Benuzzi-Mounaix, A. Ravasio, F. Dorchies, P. M. Leguay, J. Gaudin, F. Guyot, E. Brambrink, M. Koenig, S. Le Pape, and S. Mazevet, Phys. Rev. Lett. **113**, 116404 (2014).